Planta
DOI 10.1007/s00425-015-2325-1

ORIGINAL ARTICLE

Cloning and functional characterization of two monoterpene acetyltransferases from glandular trichomes of *L. x intermedia*.

Lukman S. Sarker[1] · **Soheil S. Mahmoud**[1]

Received: 1 March 2015 / Accepted: 7 May 2015

Abstract
Main conclusion **Two alcohol acetyltransferases, LiAAT-3 and LiAAT-4, from *L. x intermedia* were cloned, expressed in bacteria, and functionally characterized.**

Two monoterpene acetyltransferase cDNA clones (*LiAAT-3* and *LiAAT-4*) were isolated from *L. x intermedia* glandular trichomes, expressed in bacteria to produce, and functionally characterize the encoded proteins in vitro. The recombinant LiAAT-3 and LiAAT-4 proteins had molecular weights of ca. 47 and 49 kDa, respectively, as evidenced by SDS-PAGE. The K_m (mM) values for the recombinant LiAAT-3 and LiAAT-4 were 1.046 and 0.354 for lavandulol, 1.31 and 0.279 for geraniol, and 0.87 and 0.113 for nerol, respectively. The V_{max} (pkat/mg) values for LiAAT-3 and LiAAT-4 were 92.13 and 105.1 for lavandulol, 81.07 and 52.17 for geraniol, and 15.02 and 15.8 for nerol, correspondingly. Catalytic efficiencies (mM^{-1} - min^{-1}) for LiAAT-3 and LiAAT-4 were 0.27 and 0.85 for lavandulol, 0.19 and 0.54 for geraniol, and 0.052 and 0.4 for nerol, respectively. These kinetic properties are in the range of those reported for other plant acetyltransferases, and indicate that LiAAT-4 has a better catalytic efficiency than LiAAT-3, with lavandulol serving as the preferred substrate for both enzymes. Transcripts for both genes were abundant in *L. angustifolia* and *L. x intermedia* flowers, where monoterpene acetates are produced, and were undetectable (or present in trace quantities) in *L. latifolia* flowers, which do not accumulate significant amounts of these metabolites.

Keywords *Lavandula x intermedia* · Essential oil · Alcohol acetyltransferase · Lavandulyl acetate · Geranyl acetate · Neryl acetate

Introduction

Several species of *Lavandula* (lavenders), including *L. x intermedia*, are cultivated worldwide for their essential oils (EO), which are dominated by monoterpenes and their esters, oxides, and ketones. In particular, monoterpene esters linalyl acetate, geranyl acetate, and lavandulyl acetate occur commonly in lavenders and contribute to the characteristic aroma and flavor, and biological activities of these plants (Lis-Balchin 2002). The monoterpene esters are derived from their respective parent monoterpenes via acetylation reactions. Although the vast majority of monoterpene acetyltransferases have not been described, two BAHD-type acetyltransferases were shown to mediate the formation of geranyl acetate in rose and oil grass (Shalit et al. 2003; Sharma et al. 2013). Based on these reports, we hypothesized that BAHD acetyltransferases are also responsible for the biosynthesis of monoterpene acetates in *L. x intermedia*.

The BAHD acyltransferases are cytosolic enzymes with molecular masses ranging from 48 to 55 kDa. These enzymes, which require Acetyl Coenzyme A (Acetyl CoA) as a cofactor, contain two highly conserved motifs (D'Auria 2006). The first is the HxxxD motif, which is located near the center of the molecule, and is important for general base catalysis (D'Auria 2006; Shaw 1992; St-Pierre and De Luca 2000). The oxygen or nitrogen atom of the

✉ Soheil S. Mahmoud
soheil.mahmoud@ubc.ca

[1] Department of Biology, University of British Columbia, Okanagan Campus, 1177 Research Road, Kelowna, BC V1V 1V7, Canada

Published online: 22 May 2015

corresponding substrate is deprotonated by the histidine residue of the motif, allowing a nucleophilic attack on the carbonyl carbon of the coenzyme A thioester. This leads to the formation of a tetrahedral intermediate between the coenzyme A and the acceptor substrate. The intermediate is subsequently reprotonated to produce the free CoA and the acetylated ester or amide (D'Auria 2006). The second highly conserved region is the DFGWG motif, which is located at the carboxyl end of the protein, and is believed to have a structural role in enzymatic function (D'Auria 2006; Garvey et al. 2009; Unno et al. 2007). Nearly all functionally characterized BAHD enzymes contain both of these motifs, and deletion or modification of one or both of these motifs result in highly reduced enzyme activity (D'Auria 2006; Unno et al. 2007).

As part of an ongoing effort to complete mapping of monoterpene biosynthetic pathways in *Lavandula*, extensive genomic resources have been generated from three economically important lavender species—*L. angustifolia*, *L. x intermedia*, and *L. latifolia* (Table 1) (Demissie et al. 2012; Lane et al. 2010; Sarker et al. 2012). We identified two BAHD alcohol acetyltransferases from *L. x intermedia* glandular trichome database, and report here the cloning and functional characterization of these enzymes, which convert a variety of monoterpenes to monoterpene esters using co-enzyme A as a cofactor.

Materials and methods

Candidate selection

The construction of a cDNA library and the corresponding expressed sequence tag (EST) database from the floral glandular trichomes of mature (30 % bloomed) *L. x intermedia* flowers, and the transcript profiling experiment in various tissues of *L. angustifolia*, *L. x intermedia* and *L. latifolia* using microarray technique, were recently reported (Demissie et al. 2012; Lane et al. 2010; Sarker 2013). Probe generation, array construction, RNA labeling, array hybridization, washing, scanning, signal quantification, and data analysis for microarray experimentation were performed at the University Health Network Microarray Centre (Toronto, Canada). After analyzing the microarray data and homology-based searches, a total of four candidates (*LiAAT-1* to *LiAAT-4*) were selected for this study. Candidates were further analyzed for the presence of conserved and active motifs using the Conserved Domains module of protein structure analysis software of NCBI (http://www.ncbi.nlm.nih.gov/Structure/cdd/wrpsb.cgi), and for transit peptides using ChloroP1.1 (http://www.cbs.dtu.dk/services/ChloroP/) and Signal 3L (http://www.csbio.sjtu.edu.cn/bioinf/Signal-3L/) online software.

Relative expression assay of LiAAT

Total RNA was extracted from different lavender tissues using the RNeasy Plant Mini Kit and treated with DNase I enzyme to remove genomic DNA (Qiagen, Canada). The relative abundance of the four *LiAAT* candidates were analyzed in young leaves, and mature flowers of all three lavender species, and in glandular trichomes of *L. angustifolia* and *L. x intermedia* tissues by quantitative (qPCR), using the SteponePlus Real-Time detection system (Applied Biosystem, Canada). Complementary DNA (cDNA) for relative transcript analysis was synthesized using iScript cDNA synthesis kit (Bio-Rad) according to manufacturer's instructions. SYBR® Select Mastermix (Life Technologies, Canada) along with approximately 150 ng of cDNA as a template and 500 nM of each of the primers were used in a 10 µL reaction volume. Gene specific primers (Table 2) used in quantitative real-time

Table 1 Major monoterpenes in lavender species (English lavender, Lavandin and Spike lavender) (Lis-Balchin 2002)

	Content (%) of major terpenes in lavender oil		
	English lavender (*L. angustifolia*)	Lavandin (*L. x intermedia*)	Spike lavender (*L. latifolia*)
Linalool	10–50	20–23	26–44
Linalool acetate	12–54	19–26	0–1.5
cis and/or *trans*-Ocimen	1.0–17	1.0–3.0	0–0.3
Lavandulol and acetate	0.1–14	0.5–0.8	0.2–1.5
Camphor	0–0.2	12	5.3–14.3
1,8-Cineiol	2.1–3.0	10	25–36
α-and β-Pinene	0.02–0.3	0.6–0.9	1.6–3.6
Borneol	1.0–4.0	2.9–3.7	0.8–4.9
Limonene	0.2–0.4	0.9–1.5	1.0–2.2

Table 2 Oligonucleotides used in this study

Primer type	Target gene	primers
Full length	LiAAT-3	F-5′ AAT TGA ATT CAT GGC ATC CAC CAA AAC C 3′
		R-5′ AAA GCT CGA GCA ATG CTG AAA GAT TGA AAG 3′
	LiAAT-4	F-5′ CCC CGA ATT CAT GGC GAT GAT TAT TAC A 3′
		R-5′ CCC CCC TCG AGA GTA TCC AAT TTA TTG TA 3′
qPCR	LiAAT-3	F-5′ GCC AAA GGC ACG ATT GAT TGG 3′
		R-5′ GAG AGT CCT GGC AGC CGT AAT 3′
	LiAAT-4	F-5′ AGT TCG GCC TCT TCA TTC CG 3′
		R-5′ CTC ACC CCG TCA CTA GAT GC 3′
	Actin	F-5′ TGT GGA TTG CCA AGG CAG AGT 3′
		R-5′AAT GAG CAG GCA GCA ACA GCA 3′
	18s RNA	F-5′ GTG ACG GGT GAC GGA GAA 3′
		R-5′GAC TCA ATG AGC CCG GTA 3′

PCR (qPCR) experiments were designed manually as LiAAT-1, LiAAT-2, and LiAAT-3 share above 80 % nucleotide sequence similarity. Primer sequences were analyzed for hairpin, self-dimer, and hetero-dimer formation using IDT primer quest software (http://www.idtdna.com/Scitools/Applications/Primerquest/). The following program was used for qPCR: initial heat-labile Uracil-DNA Glycosylase (UDG) activation step at 50 °C for 2 min, denaturation at 95 °C for 2 min, and 50 cycles of 3 s at 95 °C and 30 s at 60 °C. Following threshold-dependent cycling, melting dissociation was performed from 60 to 95 °C at 0.3 °C/s melt rates with a smooth curve setting. PCR efficiency was calculated using LinRegPCR for all the primers used in this experiment, and updated in the SteponePlus data analysis software (Ruijter et al. 2009). Normalized expression values ($\Delta\Delta^{CT}$) of *LiAAT* candidates were calculated by DataAssist^{TM} software (Life technologies, Canada) using β-actin and 18S RNA as reference genes.

Treated RNA was reverse transcribed with Oligo-dT (80 μM) and random hexamers (40 μM) (Custom oligos, IDT Canada) using *M-MuLV* reverse transcriptase enzyme (New England Biolabs, Canada), following manufacturer's protocol. Transcriptional activities of *LiAAT-3* and *LiAAT-4* were analyzed in the tissues described above by standard PCR using specific primers (Table 2) with *Taq* DNA Polymerase (New England Biolabs, Canada). The following PCR program was used: initial denaturation at 95 °C for 5 min, followed by 95 °C for 1 min, 60 °C for 30 s and 72 °C for 30 s for 25/30 cycles with a final elongation at 72 °C for 5 min.

Recombinant protein expression and purification

The coding regions of selected sequences were amplified from *L. x intermedia* glandular trichome cDNA using appropriate primers (Table 2) and *iproof* HiFi taq polymerase (Bio-rad, Canada). The PCR program used was initial denaturation at 95 °C for 5 min, followed by 95 °C for 1 min, 52 °C for 30 s, and 72 °C for 1.5 min for 35 cycles with a final elongation at 72 °C for 5 min. PCR products were purified using a Gel extraction/PCR purification kit (Omega Bio-Tek, USA). The purified PCR products were inserted in the XhoI/EcoRI site of the pGEX4T-1 bacterial expression vector fused to the coding sequences for glutathione *S*-transferase (GST). The resulting constructs were transformed into *E. coli* BL21(DE3)plysS cells (EMD Chemicals, Darmstadt, Germany) to allow production of the recombinant proteins. Cells were grown and induced at 20 °C with isopropyl-β-D-thiogalactopyranoside (IPTG) at a final concentration of 0.5 mM for 12–14 h in Luria–Bertani (LB) media supplemented with 100 mg/L ampicillin and 34 mg/L chloramphenicol. The induced cells were chilled on ice for 15–20 min, collected by centrifugation at 3220*g* and 4 °C for 20 min, and stored at −80 °C overnight. The harvested cells were thawed and resuspended in GST wash buffer (43 mM Na_2HPO_4, 14.7 mM KH_2PO_4, 1.37 M NaCl, 27 mM KCl, pH 7.3) supplemented with 1 mM protease inhibitor phenylmethanesulfonylfluoride (PMSF). Cells were further sonicated on ice using a Sonic Dismembrator Model 100 (Fisher Scientific, Ottawa, ON, Canada) to complete bacterial membrane disruption after the freeze thaw cycle. The lysate was centrifuged (10,000*g*, 20 min) and incubated for 90 min with GST bind resin previously equilibrated with GST wash buffer on ice. After centrifugation (600*g*, 5 min), the supernatant was discarded and the resin was washed three times with 10 volumes of GST wash buffer. Thrombin (EMD Chemicals, Darmstadt, Germany) was applied to the resin containing recombinant protein at 1 U/mg concentration for 12 h at 4 °C in a tilted rocking platform. Treated resin was centrifuged at 500*g* for 2 min and the supernatant was collected carefully for the recombinant protein. GST elution buffer (50 mM Tris–Cl, pH 8.0, 10 mM reduced glutathione) was also treated to collect residual protein

fragments for SDS-PAGE analysis. Protein samples were filtered through an Amicon column (30 K cut off) to increase the protein concentration by lowering the total volume. Protein samples were stored in protein storage buffer (50 mM Tris, 1 mM DTT, 1 mM EDTA, 0.5 mg BSA, 10 mM NaCl, and 15 % glycerol at pH 7.5). Protein concentration was determined by the Bradford method.

Enzymatic assay and kinetic study

Initial enzyme activity was studied in 0.5 mL reaction volume with protein storage buffer, 2 mM substrate (geraniol, lavandulol, and linalool), 0.2 mM acetyl CoA, and 10 µg of protein. After overnight incubation at 30 °C with 80 rpm shaking, assay products were extracted into 0.5 mL pentane and concentrated ~50 times before analysis by gas chromatography and mass spectometry (GCMS) (see below). Negative controls were performed using protein extracted from bacteria harboring the empty vector (without insert), maintaining all other condition of the regular experiment. For linear kinetics study, assays were performed at five different time points: 10, 30, 60, 90, and 120 min. The optimum temperature was determined from a set of reactions performed at 25–37 °C for 30 min. The optimum pH was determined by performing assays at pH 5.5–10.0 using different compatible buffers using the method stated above. All assays were performed in duplicate or triplicate for statistical significance. Reaction assays contained camphor (1 mg/mL) as an internal standard to quantify the amount of product formed.

The Michaelis–Menten saturation curve was constructed using enzyme assays (n = 3) performed at optimum temperature (32 °C) and pH (8.0) for 30 min in 0.5 mL reaction volume containing 50 mM sodium phosphate buffer, 250 nM enzyme, 0.2 mM Acetyl CoA, and substrate concentration from 10 µM to 5 mM. Reactions were terminated by simple mixing followed by freezing at −80 °C. Assay products were recovered in 0.5 mL pentane and analyzed by GCMS, as discussed below. Kinetic parameters were determined from a Michaelis–Menten saturation curve constructed using SigmaPlot software version v.10.00 (Systat Software, Germany).

GCMS analysis

Assay products were analyzed using a Varian 3800 Gas Chromatographer coupled to a Saturn 2200 Ion Trap mass detector. The instrument was equipped with a 30 m × 0.25 mm capillary column coated with a 0.25 µm film of acid-modified polyethylene glycol (ECTM 1000, Altech, Deerfield, IL, USA), and a CO_2 cooled 1079 Programmable Temperature Vaporizing (PTV) injector (Varian Inc., USA). Samples were injected on-column at 40 °C. The oven temperature was initially maintained at 40 °C for 1 min, raised to 100 °C at a rate of 30 °C/min, then set to 150 °C at a rate of 6 °C/min, then set to 230 °C at a rate of 35 °C/min, and finally held at 230 °C for 2 min. The carrier gas (helium) flow rate was set to 1 mL/min. Identification of the products was confirmed by comparing their retention time and mass spectra to those of authentic standards (from our collection) analyzed under the same condition. EO constituents were identified by comparison of obtained mass spectra to those of authentic standards, or to those in the NIST library.

Multiple sequence alignment and phylogenetic tree analysis

Amino acid sequences for LiAAT candidates were blasted against those in the NCBI database using the BLASTp function to identify the closest homologs, which were analyzed by multiple sequence alignment using the default parameters of the ClustalW tools available at the EBI platform (http://www.ebi.ac.uk/Tools/msa/clustalw2/). The phylogenetic tree was created using neighbor-joining and boostrap analysis of Geneious Tree Builder module (Geneious 5.0.3 software, Auckland, New Zealand).

Accession number

The coding sequences for *LiAAT-3* (Accession # KM275343) and *LiAAT-4* (Accession # KM275344) have been submitted to NCBI.

Results

Candidate selection

Construction of a cDNA library and the corresponding expressed sequence tag (EST) database from the secretory cells of *L. x intermedia* flower glandular trichomes were previously reported (Demissie et al. 2012). The annotated EST database was initially searched using the keyword "acetyltransferase" to identify putative alcohol acetyltransferase homologs. The selected candidates were further screened by comparing their sequences to those of known alcohol acetyltransferases (AAT) present in online databases. The initial search yielded a total of 117 ESTs as putative acetyltransferases. Among these, two ESTs were singleton while the remaining 115 ESTs formed eight contigs. Subsequent search, based on GO annotation, revealed that four contigs were potentially viable terpene alcohol acetyltransferases, while others corresponded to histone acetyltransferase, amino acid acyltransferase, and dihydrolipoamide acyltransferase, among others.

The four selected contigs, LiAAT-1, LiAAT-2, LiAAT-3, and LiAAT-4, contained six, 35, 20, and 35 ESTs, respectively (Table 3), and produced transcripts with complete ORFs for *LiAA-1–LiAA-4* candidates.

Given that the floral EOs of *L. x intermedia* and *L. angustifolia* contain substantial amounts of monoterpene acetates, we anticipated strong expression of EO-related acetyltransferase in the floral tissue of these plants. However, we did not expect to observe strong expression of these genes in flowers of *L. latifolia*, which do not accumulate significant amounts of monoterpene acetates (Herraiz-Penalver et al. 2013; Lis-Balchin 2002; Sarker 2013). Our microarray analysis experiments indicated that transcripts corresponding to *LiAAT* candidates were more abundant (by 1.9, 1.4, 18.5, and 18 fold for *LiAAT-1*, *LiAAT-2*, *LiAAT-3*, and *LiAAT-4*, respectively) in *L. x intermedia* as compared to *L. latifolia* floral tissue (Table 3). Similarly, transcript levels for all candidates were higher in newly opened flowers (anthesis stage), which accumulate monoterpene acetates, compared to unopened buds, which do not produce these compounds (Table 3). A similar expression pattern was observed for *LiAAT-3* and *LiAAT-4* in *L. angustifolia* flowers. However, transcripts for *LiAAT-1* and *LiAAT-2* were 52 and 11 fold down-regulated in *L. angustifolia* compared to *L. latifolia* floral tissue, indicating that these sequences are not likely to be involved in EO metabolism. Based on these observations, *LiAAT-3* and *LiAAT-4* were selected for further analysis.

Sequence analysis

The open reading frames (ORF) of *LiAAT-3* and *LiAAT-4* consist of 1344 and 1254 bp, coding for proteins of 447 and 417 amino acids with predicted molecular weights of 50.27 and 47.57 kDa, respectively. Proteins were predicted to be cytosolic since none of the ORFs encoded a transit peptide. Intracellular trafficking of isoprenoid metabolites is known to occur in different organisms. For example, the intermediates involved in the biosynthesis of the monoterpene menthol in peppermint oil glands are believed to move around the cell for hydroxylation and isomerization reactions (Turner et al. 2000). LiAAT-3 and LiAAT-4 proteins were highly homologous to alcohol acetyltransferases from strawberry and apple fruit (FaSAAT, MpAAT), and included all the conserve motifs present in typical plant alcohol acetyltransferases, specifically HxxxD and DFGWG motifs (D'Auria 2006) (Fig. 1). However, in LiAAT-3, aspartic acid (D) and phenylalanine (F) of DFGWG motif were replaced with glutamic acid (E) and valine (V), respectively. LiAAT-4 contained two HxxxD motifs separated by 29 amino acids, and an unaltered DFGWG motif at the C-terminal end (Fig. 1).

Heterologous protein expression and enzymatic assay

The coding sequences of *LiAAT-3* and *LiAAT-4* candidates were cloned into pGEX4T-1 vector using EcoRI and XhoI restriction sites, which allowed for the production of N-terminal GST tagged recombinant proteins. The GST tag was removed by thrombin digestion, and the purified enzymes were used in enzymatic assays using monoterpenoid alcohols, as substrates. Initially, 10 µg of each enzyme was used in a reaction containing 2 mM of linalool, geraniol, and lavandulol as substrate and incubated overnight at 30 °C. The reaction was terminated, and assay products were extracted in 0.5 mL pentane after storing reaction vials at −80 °C, allowing volatile compounds to settle. Assay products were concentrated around 50 times before analysis by GCMS. LiLAAT-3 and LiAAT-4 both produced significant amounts of respective esters from geraniol and lavandulol, but not from linalool (Fig. 2). A small amount of linalyl acetate was also present in all assays, including the negative control, indicating that it was most likely a contaminant of the substrate (linalool) preparation (not shown).

LiAAT kinetic studies

The kinetic properties were determined at a pH of 8.0, temperature of 32 °C, acetyl-CoA concentration of 0.2 mM, and substrate concentrations of 10 µM–5 mM. Significant substrate inhibition was observed at the 5 mM point, therefore was not included in the kinetic analysis reported in Fig. 3.

Table 3 Microarray analysis

Candidate	# of ESTs	LI vs LA	LI vs LL	LA vs LL	Bud vs Anth (LI-gland)
LiLAT-1	6	Up-44	Up-1.89	Down-52	Down-4
LiLAT-2	35	Up-2.4	Up-1.39	Down-11	Down-6
LiLAT-3	20	Up-1.47	Up-18.5	Up-20.79	Down-6
LiLAT-4	35	No change	Up-18	Up-18	Down-7

LA = *L. angustifolia; LI* = *L. x intermedia*; *LL* = *L. latifolia*; *LI-gland* = glandular trichomes from *L. x intermedia* bud and anthesis flower developmental stages. Unless otherwise stated, 30 % bloomed flower tissues were used for all other species; *up* = up-regulation, *down* = down regulation in their respective tissues

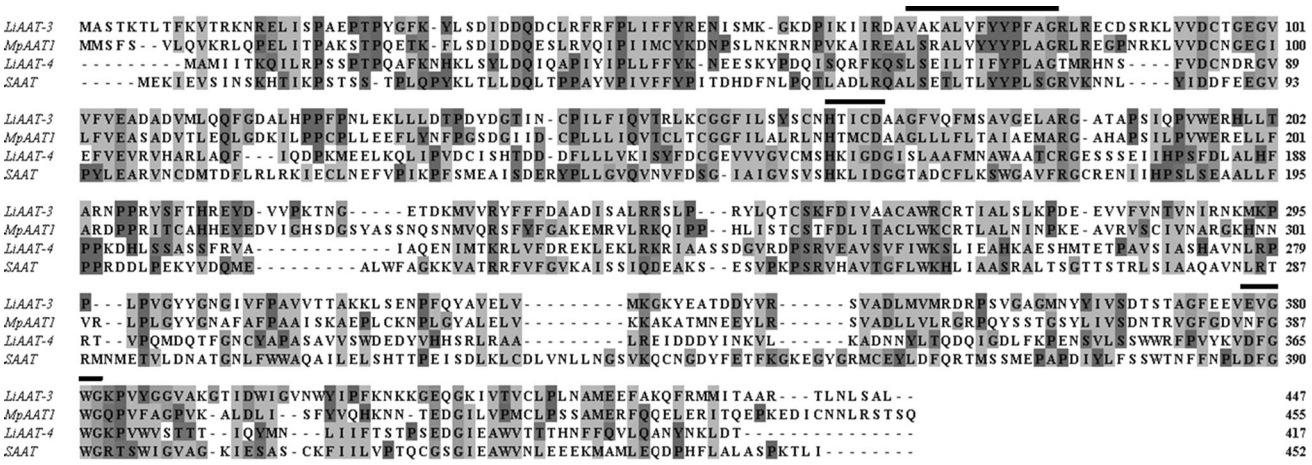

Fig. 1 Multiple sequence alignment of *LiAAT-3* and *LiAAT-4* with respect to their closest alcohol acetyltransferase homolog *MpAAT1*—*Malus pumila* (pumila-) alcohol acyltransferase, and *SAAT*-strawberry alcohol acetyltransferase. *Black bar* indicate the conserve motifs HxxxD and DFGWG

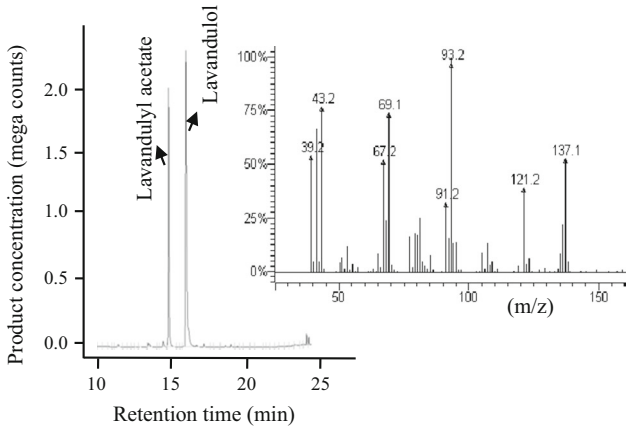

Fig. 2 GCMS analysis of assay products formed in LiAAT-3 and LiAAT-4 enzymatic assays. As an example, GCMS chromatogram of reaction products formed from lavandulol by LiAAT-4 is shown. Mass spectrum of lavandulol acetate also included

The Michaelis–Menten enzyme saturation curve was generated using the hyperbolic enzyme kinetics analysis module of the SigmaPlot software. The K_m of LiAAT-3 for geraniol, lavandulol, and nerol was calculated as 1.31, 1.05, and 0.87 mM, respectively. The V_{max} of the enzyme for the same substrates was 81.07, 92.13, and 15.02 pkat/mg, respectively (Fig. 3). Turnover number (k_{cat}) and catalytic efficiency (k_{cat}/K_m) of LiAAT-3 were calculated for geraniol, lavandulol, and nerol with values of 0.245, 0.278, and 0.045 min^{-1} and 0.186, 0.266, and 0.052 mM^{-1} min^{-1}, correspondingly. Similarly, kinetic parameters of LiAAT-4 candidate were calculated for geraniol, lavandulol, and nerol. For these substrates K_m was 0.279, 0.354, 0.118 mM, and V_{max} was 52.17, 105.1, and 15.8 pkat/mg, respectively (Fig. 3). Turnover number (k_{cat}) and catalytic efficiency (k_{cat}/K_m) of LiAAT-4 for geraniol, lavandulol, and nerol were found to be 0.151, 0.30, and 0.045 min^{-1} and 0.539, 0.848, and 0.40 mM^{-1} min^{-1}, respectively (Table 4).

Tissue specific regulation of *LiAAT*

The expression patterns of LiAAT-3 and LiAAT-4 transcripts in leaf, flower, and glandular trichomes of *L. x intermedia* and in *L. angustifolia*, and flower tissues of *L. latifolia* were evaluated by standard and qPCR. The results of the standard PCR assay revealed that transcripts for both candidates were highly concentrated in *L. x intermedia* and *L. angustifolia* floral glandular trichomes (Fig. 4). Transcript levels were quantitated in flowers relative to leaves for the qPCR study. The results of the qPCR experiment confirmed these findings, demonstrating that LiAAT-3 transcripts were up-regulated by 118 and 5866 fold in flowers and glandular trichomes of *L. angustifolia*, respectively, and by 1.3 and 49 fold in flowers and glandular trichomes of *L. x intermedia*, respectively. LiAAT-4 transcripts were up-regulated by 83 and 1601 fold in flower and glandular trichome of *L. angustifolia*, and by 7.5 and 345 fold in flower and glandular trichome of *L. x intermedia*, respectively. LiAAT-3 transcripts were more abundant (3-fold) in *L. latifolia* flowers compared to leaf tissues, and LiAAT-4 transcripts were not detected at all (Fig. 5).

Phylogenetic tree analysis

A non-rooted phylogenetic tree was developed for all four candidates to examine their relationship with other known BAHD acetyltransferases. The tree shows all five clades of known BAHD acyltransferases (D'Auria 2006) and a new clade with one of the lavender acyltransferases (Landmann

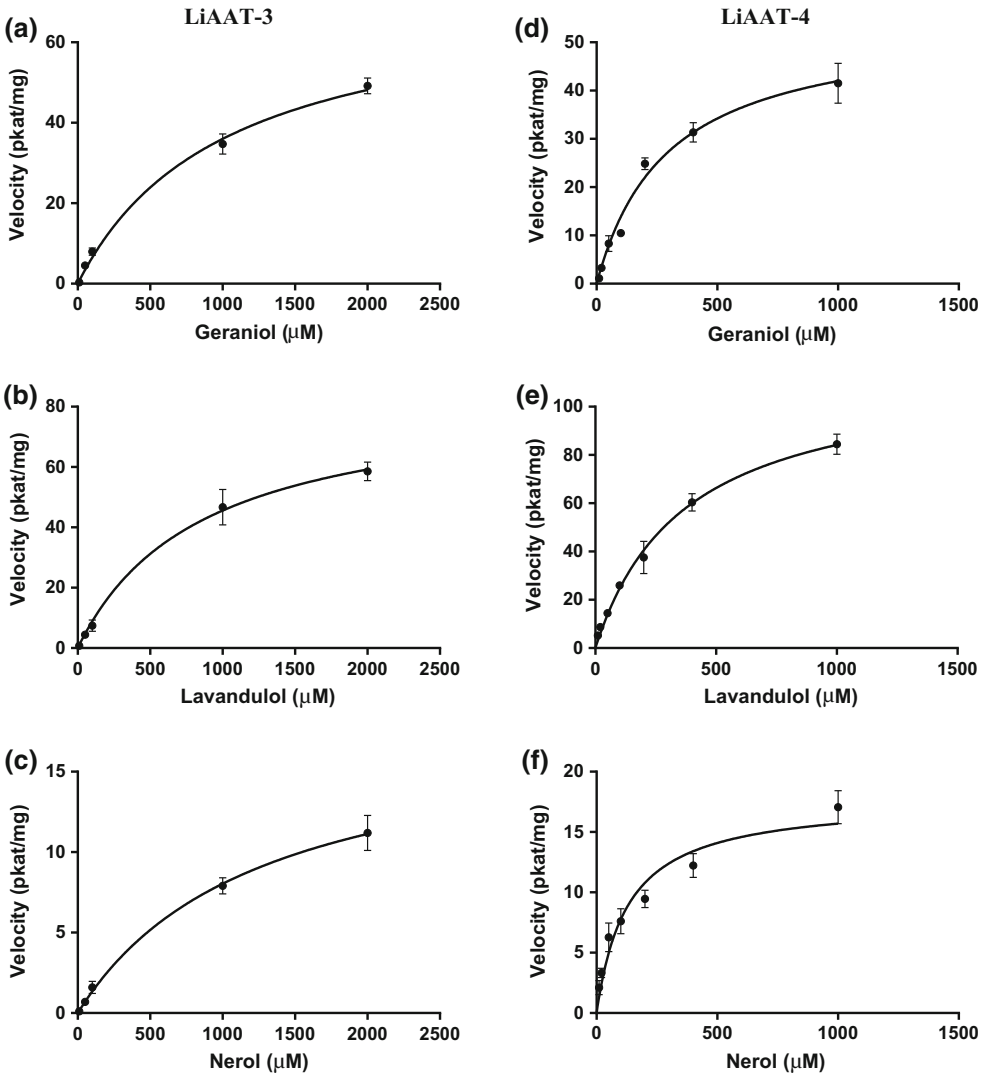

Fig. 3 Kinetic assays of for LiAAT-3 with **a** Geraniol, **b** Lavandulol, **c** Nerol, and LiAAT-4 with **d** Geraniol, **e** Lavandulol, **f** Nerol. Substrate concentration was in μM. Lavandulol was a preferred substrate for both of these candidates

et al. 2011). LiAAT1-3 falls into a subgroup of clade five (V), which consists of enzymes capable of forming the benzenoid ester benzylbenzoate. Benzyl alcohol benzoyltransferase from *Clarkia breweri* (CbBEBT) is the closest related enzyme from this subgroup with a score of 67.34 % identity with LiAAT-3. AtCHAT from *Arabidopsis thaliana* and MpAAT1 from *Malus domestica* are the two alcohol acetyltransferases from this subgroup with 60.93 and 60.15 % identity, respectively. LiAAT-4 belongs to clade three (III) with 11 additional members in it accepting a diverse range of alcohols as substrates, while Acetyl CoA is a major acyl donor. There are two subgroups in this clade, and LiAAT-4 belongs to the second subgroup closest to RsVINS, vinorine synthase of *Rauvolfia serpentine* with a score of only 40 % identity. LaAT1, a *L. angustifolia* acyltransferase clone, shares approximately 40 % sequence identity with all four LiAAT candidates and occupies clade five in the phylogram (Fig. 6).

Discussion

The EOs of most lavender species, in particular those of the commercially propagated *L. angustifolia* and *L. x intermedia* plants, contain substantial amounts of monoterpene alcohols linalool, geraniol, lavandulol, and nerol and their corresponding esters linalyl acetate, geranyl acetate, lavandulyl acetate, and neryl acetate (Lawrence 1990). However, the EO of a few species, including *L. latifolia,* do not produce a significant amount of monoterpene acetates/esters (Herraiz-Penalver et al. 2013; International Standard 2002; Lawrence 1990). The monoterpene esters impart pleasant aromas to the EO, and are among the key determinants of EO quality. For example, the finest lavender EOs, e.g., that of *L. angustifolia*, are highly enriched in linalyl acetate and other monoterpene esters, and are mostly used in the cosmetic industry or in aromatherapy (Table 1). On the other hand, lavender EOs that lack

Table 4 Kinetics data (0.2 mM acetyl CoA as co substrate)

Substrate	Parameters	LiAAT-3	LiAAT-4
Geraniol 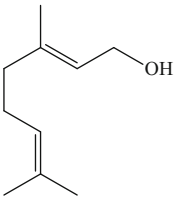	K_m (mM)	1.31	0.279
	V_{max} (pkat/mg)	81.07	52.17
	k_{cat} (min^{-1})	0.245	0.150
	k_{cat}/K_m (mM^{-1} min^{-1})	0.186	0.539
Lavandulol 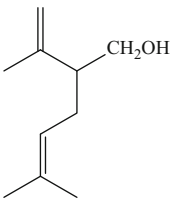	K_m (mM)	1.04613	0.354
	V_{max} (pkat/mg)	92.13	105.1
	k_{cat} (min^{-1})	0.278	0.3
	k_{cat}/K_m (mM^{-1} min^{-1})	0.266	0.848
Nerol 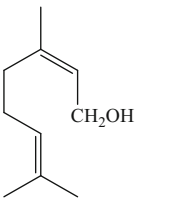	K_m (mM)	0.87	0.113
	V_{max} (pkat/mg)	15.02	15.8
	k_{cat} (min^{-1})	0.045	0.045
	k_{cat}/K_m (mM^{-1} min^{-1})	0.052	0.4

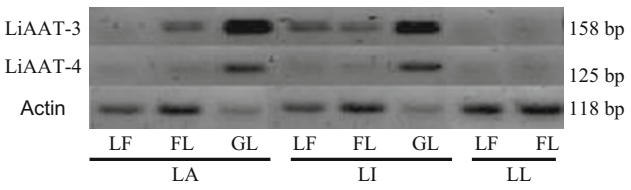

Fig. 4 Detection of transcripts for *LiAAT-3* and *LiAAT-4* by standard PCR (*LI L. x intermedia*; *LA L. angustifolia*; *LL L. latifolia*; *LF* leaf; *FL* flower; *GL* glandular trichomes). LiAAT-3 and LiAAT-4 transcripts were highly abundant in LA, and LI glandular trichomes. β-actin was used as a reference gene

monoterpene acetates, for example that of *L. latifolia*, are characterized by strong unpleasant scents due to the presence of high levels of other compounds such as camphor, and are often used in alternative medicine (Cavanagh and Wilkinson 2002). Despite the importance of monoterpene acetates, the genes responsible for the production of these metabolites in lavenders have not been described (Fig. 7).

In search of alcohol acetyltransferase genes responsible for the synthesis of monoterpene esters in *Lavandula*, a cDNA library constructed from *L. x intermedia* floral glandular trichome (Demissie et al. 2012) was screened for putative acetyltransferase homologs, and a number of cDNA candidates were identified. It is well established that

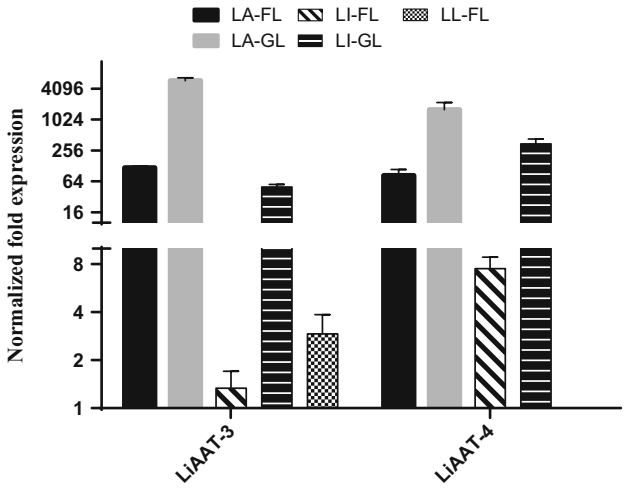

Fig. 5 Transcriptional activity of *LiAAT* candidates in different tissues of lavender species. β-actin and 18s RNA were used as a reference gene. Transcriptional activity of transcripts in flower and glandular trichome tissues were normalized against leaf of their respective plants ($n = 6$)

the expression of genes involved in monoterpene synthases is transcriptionally regulated (e.g., menthofuran synthase in peppermint leaves (Mahmoud and Croteau 2003), and linalool synthase in *L. angustifolia* flowers (Lane et al. 2010)), and that this transcriptional activity directly correlates with product (monoterpene) formation. Provided the above, and given that *L. angustifolia* and *L. x intermedia* plants accumulate monoterpene acetates but *L. latifolia* plants do not, we anticipated that monoterpene acetyltransferases of interest would be exclusively (or more strongly) expressed in *L. angustifolia* and *L. x intermedia* flowers as compared to those of *L. latifolia* plants. We therefore studied the expression pattern of the selected candidates by microarray analysis and PCR in these three closely related species. These experiments led to the identification of two differentially expressed candidates, *LiAAT-3* and *LiAAT-4*, which exhibited strong transcriptional activity in the floral tissue (in particular glandular trichomes) of *L. angustifolia* and *L. x intermedia* as compared to *L. latifolia* plants (Table 3; Figs. 4, 5).

The coding sequences for these candidates were cloned into a pGEX4T-1 expression vector and expressed in bacteria to produce the corresponding proteins. The partially purified recombinant proteins were assayed for activity using linalool, geraniol, lavandulol, and nerol as substrates, and acetyl Co-enzyme A as a cofactor. The assay reactions yielded geranyl acetate, lavandulyl acetate, and neryl acetate, but not linalyl acetate, suggesting that linalyl acetate formation is catalyzed by a different enzyme. In this context, the cell-free extracts of glandular trichomes of lemon plants were able to catalyze the conversion of linalool to linalyl acetate, indicating that an

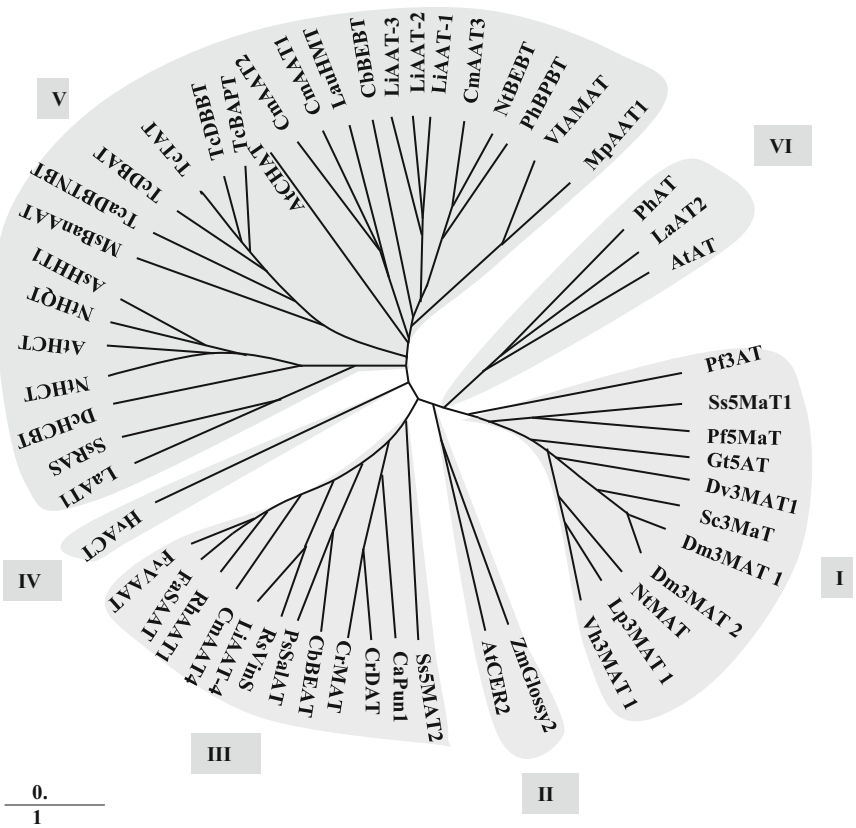

Fig. 6 Phylogenetic tree analysis of BAHD acyltransferases including LiAAT-1-4. The tree was constructed by neighbor-joining and bootstrap distance analysis (adapted from D'Auria 2006; Landmann et al. 2011). Candidates included that have been characterized by either genetic mutant screening or biochemical assay. AsHHT1, *Avena sativa* hydroxycinnamoyl-CoA: hydroxyanthranilate-*N*-hydroxycinnamoyltransferse (BAC78633); AtAT, *Arabidopsis thaliana* acyltransferase (NP_197782); AtCER2, *A. thaliana* CER2-protein, biosynthesis of C30-waxes (AAM64817)1; AtCHAT, *A. thaliana* (Z)-3-hexen-1-ol-*O*-acetyltransferase (AAN09797); AtHCT, *A. thaliana* hydroxycinnamoyl-CoA; shikimate/quinate hydroxycinnamoyltransferase (NP_199704); CaPun1, *Capsicum annum* Pun1-Protein, biosynthesis of capsaicin (AAV66311); CbBEAT, *Clarkia breweri* benzyl alcohol-*O*-acetyltransferase (AAC18062); CbBEBT, *C. breweri* benzoyl-CoA: benzyl alcohol-*O*-benzoyltransferase (AAN09796), CmAAT1-4, *Cucumis melo* alcohol acyltransferase (CAA94432, AAl77060, AAW51125, AAW51126); CrDAT, *Catharanthus roseus* deacetylvindolin-4-*O*-acetyltransferase (AAC99311); CrMAT, *C. roseus* minovincinin-19-hydroxy-*O*-acetyltransferase (AAO13736); DcHCBT: *Dianthus caryophyllus* anthranilate-*N*-hydroxycinnamoyl/benzoyltransferase (CAB06430); Dm3MAT1-2, *Dendramthema x morifolium* anthocyanidine-3-*O*-glucosid-6″-*O*-malonyl-transferase (AAQ63615, AAQ63616); Dv3MAT, *Dahlia variabilis* malonyl-CoA: anthocyanidine-3-*O*-glucosid-6″-*O*-malonyltransferase (AAO12206); FaSAAT, *Fragaria x ananassa* (strawberry-) alcohol acyltransferase (AAG13130); FvVAAT, *Fragaria vesca* alcohol acyltransferase (CAC09062); Gt5AT, *Gentiana triflora* anthocyanin-5-aromatic acyltransferase (BAA74428); HcACT, *Hordeum vulgare* agmatine-coumaroyltransferase (AAO73071); LaAT1 and LaAt2, *L. angustifolia* acyltransferase 1 and 2 (ABI48360 and ABI48361); Lp3MAT1, *Lamium purpureum* malonyl-CoA: flavonol-3-*O*-glucosid-6″-*O*-malonyl- transferase (AAS77404); LuaHMT/HLT, *Lupinus albus* tigloyl-CoA; 13α-hydroxymultiflorin/13α-hydroxy-lupanin-*O*-tigloyltransferase (BAD89275); MpAAT1, *Malus pumila* (pumila-) alcohol acyltransferase (AAU14879); MsBanAAT, *Musa sapientum* (banana-) alcohol acyltransferase (CAC09063); NtBEBT, *Nicotiana tabacum* benzoyl-CoA, benzyl alcohol-*O*-benzoyltransferase (AAN09798); NtHCT, *N. tabacum* hydroxycinnamoyl-CoA, shikimate/quinate hydroxycinnamoyltransferase (CAD47830); NtHQT, *N. tabacum* hydroxycinnamoyl-CoA: quinate hydroxycinnamoyltransferas (CAE46932); NtMAT, *N. tabacum* malonyl-CoA: flavonoid/naphthol-glucosid-acyltransferase (BAD93691); Pf3AT, *Perilla frutescens* hydroxy cinnamoyl-CoA: anthocyanin-3-*O*-glucosid-6″-*O*-acyltransferase (BAA93475); Pf5MAT, *P. frutescens* anthocyanin-5-*O*-glucosid-6″-*O*-malonyltransferase (AAL50565); PhAT, *Petunia hybrida* acyltransferase (BAA93453); PhBPBT, *P. hybrida* benzoyl-CoA: benzyl alcohol/phenylethanol-benzoyltransferase (AAU06226); PsSaIAT, *Papaver somniferum* salutaridinol-7-*O*-acetyltransferase (AAK73661); RhAAT1, *Rosa hybrida* alcohol acetyltransferase (AAW31948); RsVinS, *Rauwolfia serpentina* vinorinsynthase (CAD89104); Sc3MaT: *Senecia cruentus* malonyl-CoA: anthocyanidin-3-*O*-glucosid-6″-*O*-malonyl-transferase (AAO38058) Ss5MAT1: *Salvia splendens* malonyl-CoA; anthocyanin-5-*O*-glucosid-6″-*O*-malonyltransferase (AAL50566); SsRAS: *Solenostemon scutellarioides* rosmarinic acid synthase (CAK55166); TcaDBTNBT: *Taxus Canadensis* 3′-*N*-debenzoyltaxol-*N*-benzoyltransferase (AAM75818); TcBAPT, *Taxus cuspidata* baccatin-III-*O*-phenylpropanoyltransferase (AAL92459); TcDBAT, *T. cuspidata* 10-deacetylbaccatin-III-10-*O*-acetyltransferase (AAF27621); TcDBBT, *T. cuspidata* 2-debenzoyl-7, 13-diacetylbaccatin-III-*O*-benzoyltransferase (Q9FPW3); TcTAT, *T. cuspidata* taxa-4(20),11(12)-dien-5α-ol-*O*-acetyltransferase (AAF34254); Vh3MAT1, *Verbena x hybrida* malonyl-CoA: flavonol-3-*O*-glucosid-6″-*O*-malonyltransferase (AAS77404); VIAMAT, *Vitis labrusca* anthranoyl-CoA:methanolacyltransferase (AAW22989); ZmGlossy2, *Zea mays* Glossy2-protein, biosynthesis of C32-waxes (CAA61258). Clade VI candidates have not been characterized

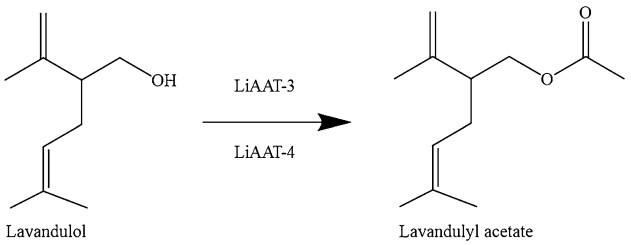

Fig. 7 Proposed pathway for Lavandulyl acetate biosynthesis in lavender

enzyme capable of catalyzing this reaction exists (Zaks et al. 2008). Given that linalool is a tertiary alcohol (other monoterpenes studied here are primary or secondary alcohols), it is possible that the linalool acetyltransferase is different in structure and mechanism of action than enzymes reported here (Aharoni et al. 2000; Beekwilder et al. 2004; Zaks et al. 2008).

The optimum pH and temperature for LiAAT-3 and LiAAT-4 were in the range of alcohol acetyltransferases reported previously (Landmann et al. 2011; Sharma et al. 2013) and were determined to be 8.0–8.5 and 30–32 °C, respectively. Both enzymes demonstrated linear catalytic activity from 10 to 120 min. Based on the kinetics data, LiAAT-4 has a much lower K_m (mM) value than LiAAT-3 for all the substrates used in this experiment. However, both enzymes had similar V_{max} values for all substrates except for geraniol, in which case V_{max} was higher for LiAAT-3 (81.07 pkat/mg) than LiAAT-4 (52.17 pkat/mg) (Table 4). Therefore, LiAAT-4 had a better catalytic efficiency than LiAAT-3 with a fold difference of 2.9, 3.19, and 7.7 for geraniol, lavandulol, and nerol, respectively. Among these three substrates, lavandulol was a preferred substrate compared to geraniol and nerol. The catalytic efficiency for lavandulol was approximately 1.5 fold higher than that of geraniol for both enzymes. Also, geraniol was the preferred substrate compared to nerol, as the catalytic efficiencies of LiAAT-3 and LiAAT-4 were 3.1 and 1.35 fold higher for the former substrate. Kinetic parameters of LiAAT-3 and LiAAT-4 are in the range of those reported for previously cloned or biochemically characterized alcohol acyltransferase genes from a number of different plants (Aharoni et al. 2000; Beekwilder et al. 2004; El-Sharkawy et al. 2005; Shalit et al. 2003). In addition, enzymatic activity of FvVAAT, CmAAT-4, CbBEBT, VpAAT1 for geraniol and nerol were reported to be in the range of 10–3451 pkat/mg in the presence of acetyl CoA (Balbontin et al. 2010; Beekwilder et al. 2004; D'Auria et al. 2002; El-Sharkawy et al. 2005).

LiAAT-3 and LiAAT-4 were found to be associated with clade V and clade III after a non-rooting phylogenetic analysis with other characterized acetyltransferases from different plants (Fig. 6). Although these proteins contain both conserved motifs found in acyltransferases, the aspartic acid of DFGWG motif was replaced by glutamic acid (E^{378}) in LiAAT-3. It has been reported that HxxxD and DFGWG motifs are highly conserved in all acyltransferase proteins, and alterations of these motifs result in reduced enzyme activity (Bayer et al. 2004; D'Auria 2006; Suzuki et al. 2002; Unno et al. 2007). This could be the reason for the lower enzymatic activity of LiAAT-3 compared to LiAAT-4. In this context, other poorly active or inactive acyltransferase homologs (e.g., AtCER2 and ZmGlossy2) containing glutamic acid instead of aspartic acid in DFGWG motif have been previously reported (Tacke et al. 1995; Xia et al. 1996). In addition, a third conserved motif, LSxTLxxxYxxxG (Aharoni et al. 2000; El-Sharkawy et al. 2005; Gonzalez et al. 2009; Sharma et al. 2013), which is less conserved among acyltransferase genes, is present in LiAAT-4 with a modification of threonine^{73} to isoleucine^{73}. Only leucine^{74}, tyrosine^{78} and glycine^{82} are present in LiAAT-3 for the third motif.

In conclusion, we have cloned and functionally characterized two alcohol acetyltransferases from *L. x intermedia* glandular trichomes. Both enzymes are capable of synthesizing geranyl acetate, lavandulyl acetate, and neryl acetate from their respective monoterpene substrates, although both enzymes exhibit a preference for lavandulol as a substrate. Neither enzyme was able to convert linalool to linalyl acetate, which is a major EO constituent in some lavender species, indicating that a different acetyltransferase enzyme is likely involved in the production of linalyl acetate. The cloning of these acetyltransferases has significant implications in understanding the biology of essential oil formation in higher plants and enables future experiment aimed at improving EO quality and yield in lavenders through metabolic engineering and targeted breeding programs.

Author contribution SM and LS contributed to experimental design. LS conducted all experiments related to this research.

Acknowledgments This work was supported through grants or in-kind contributions to SSM by UBC, Natural Sciences and Engineering Research Council of Canada, and Investment Agriculture Foundation of British Columbia. We are grateful to Dr. Mark Rheault of UBC Okanagan for his support to use Geneious 5.0.3 software. We also thank Felisha Truong for her editorial assistance.

Compliance with ethical standards There were no humans or animals used in this research. All authors have read and approve of the manuscript, and there are no conflicts of interest.

References

Aharoni A, Keizer LCP, Bouwmeester HJ, Sun ZK, Alvarez-Huerta M, Verhoeven HA, Blaas J, van Houwelingen AMML, De Vos

RCH, van der Voet H, Jansen RC, Guis M, Mol J, Davis RW, Schena M, van Tunen AJ, O'Connell AP (2000) Identification of the SAAT gene involved in strawberry flavor biogenesis by use of DNA microarrays. Plant Cell 12:647–661

Balbontin C, Gaete-Eastman C, Fuentes L, Figueroa CR, Herrera R, Manriquez D, Latche A, Pech J, Alejandra Moya-Leon M (2010) VpAAT1, a gene encoding an alcohol acyltransferase, is involved in ester biosynthesis during ripening of mountain papaya fruit. J Agric Food Chem 58:5114–5121

Bayer A, Ma XY, Stockigt J (2004) Acetyltransfer in natural product biosynthesis—functional cloning and molecular analysis of vinorine synthase. Bioorg Med Chem 12:2787–2795

Beekwilder J, Alvarez-Huerta M, Neef E, Verstappen F, Bouwmeester H, Aharoni A (2004) Functional characterization of enzymes forming volatile esters from strawberry and banana. Plant Physiol 135:1865–1878

Cavanagh HMA, Wilkinson JN (2002) Biological activities of lavender essential oil. Phytotherapy Research 16:301–308

D'Auria JC (2006) Acyltransferases in plants: a good time to be BAHD. Curr Opin Plant Biol 9:331–340

D'Auria J, Chen F, Pichersky E (2002) Characterization of an acyltransferase capable of synthesizing benzylbenzoate and other volatile esters in flowers and damaged leaves of *Clarkia breweri*. Plant Physiol 130:466–476

Demissie ZA, Cella MA, Sarker LS, Thompson TJ, Rheault MR, Mahmoud SS (2012) Cloning, functional characterization and genomic organization of 1,8-cineole synthases from *Lavandula*. Plant Mol Biol 79:393–411

El-Sharkawy I, Manriquez D, Flores F, Regad F, Bouzayen M, Latche A, Pech J (2005) Functional characterization of a melon alcohol acyl-transferase gene family involved in the biosynthesis of ester volatiles. Identification of the crucial role of a threonine residue for enzyme activity. Plant Mol Biol 59:345–362

Garvey GS, McCormick SP, Alexander NJ, Rayment I (2009) Structural and functional characterization of TRI3 trichothecene 15-*O*-acetyltransferase from *Fusarium sporotrichioides*. Protein Sci 18:747–761

Gonzalez M, Gaete-Eastman C, Valdenegro M, Figueroa CR, Fuentes L, Herrera R, Alejandra Moya-Leon M (2009) Aroma development during ripening of *Fragaria chiloensis* fruit and participation of an alcohol acyltransferase (FcAAT1) gene. J Agric Food Chem 57:9123–9132

Herraiz-Penalver D, Angeles Cases M, Varela F, Navarrete P, Sanchez-Vioque R, Usano-Alemany J (2013) Chemical characterization of *Lavandula latifolia* Medik. essential oil from Spanish wild populations. Biochem Syst Ecol 46:59–68

International Standard (2002) ISO 3515:2002 Oil of lavender (*Lavandula angustifolia* Mill)

Landmann C, Huecherig S, Fink B, Hoffmann T, Dittlein D, Coiner HA, Schwab W (2011) Substrate promiscuity of a rosmarinic acid synthase from lavender (*Lavandula angustifolia* L.). Planta 234:305–320

Lane A, Boecklemann A, Woronuk GN, Sarker L, Mahmoud SS (2010) A genomics resource for investigating regulation of essential oil production in *Lavandula angustifolia*. Planta 231:835–845

Lawrence BM (1990) Progress in Essential Oils. Perfum Flavor 15(57–60):63–65

Lis-Balchin M (2002) Lavender: the genus *Lavandula*. Taylor and Francis, London

Mahmoud S, Croteau R (2003) Menthofuran regulates essential oil biosynthesis in peppermint by controlling a downstream monoterpene reductase. Proc Natl Acad Sci USA 100: 14481–14486

Ruijter JM, Ramakers C, Hoogaars WMH, Karlen Y, Bakker O, van den Hoff MJB, Moorman AFM (2009) Amplification efficiency: linking baseline and bias in the analysis of quantitative PCR data. Nucleic Acids Res 37:e45

Sarker LS (2013) Cloning of *Lavandula* essential oil biosynthetic genes. M.Sc thesis, University of British Columbia. http://hdl.handle.net/2429/43964

Sarker LS, Galata M, Demissie ZD, Mahmoud SS (2012) Molecular cloning and functional characterization of borneol dehydrogenase from the glandular trichomes of *Lavandula x intermedia*. Arch Biochem Biophys 528(2):163–170

Shalit M, Guterman I, Volpin H, Bar E, Tamari T, Menda N, Adam Z, Zamir D, Vainstein A, Weiss D, Pichersky E, Lewinsohn E (2003) Volatile ester formation in roses. Identification of an acetyl-coenzyme A. Geraniol/citronellol acetyltransferase in developing rose petals. Plant Physiol 131:1868–1876

Sharma PK, Sangwan NS, Bose SK, Sangwan RS (2013) Biochemical characteristics of a novel vegetative tissue geraniol acetyltransferase from a monoterpene oil grass (Palmarosa, *Cymbopogon martinii* var. Motia) leaf. Plant Sci 203:63–73

Shaw WV (1992) Chemical anatomy of antibiotic-resistance—chloramphenicol acetyltransferase. Sci Prog 76:565–580

St-Pierre B, De Luca V (2000) Evolution of acyltransferase genes: origin and diversification of the BAHD superfamily of acyltransferases involved in secondary metabolism. Evol Metabol Pathw 34:285–315

Suzuki H, Nakayama T, Yonekura-Sakakibara K, Fukui Y, Nakamura N, Yamaguchi M, Tanaka Y, Kusumi T, Nishino T (2002) cDNA cloning, heterologous expressions, and functional characterization of malonyl-coenzyme A : anthocyanidin 3-*O*-glucoside-6″-*O*-malonyltransferase from dahlia flowers. Plant Physiol 130:2142–2151

Tacke E, Korfhage C, Michel D, Maddaloni M, Motto M, Lanzini S, Salamini F, Doring HP (1995) Transposon tagging of the maize Glossy2 locus with the transposable element En/Spm. Plant J 8:907–917

Turner GW, Gershenzon J, Croteau RB (2000) Development of peltate glandular trichomes of peppermint. Plant Physiol 124:665–679

Unno H, Ichimaida F, Suzuki H, Takahashi S, Tanaka Y, Saito A, Nishino T, Kusunoki M, Nakayama T (2007) Structural and mutational studies of anthocyanin malonyltransferases establish the features of BAHD enzyme catalysis. J Biol Chem 282:15812–15822

Xia YJ, Nicolau BJ, Schnable PS (1996) Cloning and characterization of CER2, an *Arabidopsis* gene that affects cuticular wax accumulation. Plant Cell 8:1291–1304

Zaks A, Davidovich-Rikanati R, Bar E, Inbar M, Lewinsohn E (2008) Biosynthesis of linalyl acetate and other terpenes in lemon mint (*Mentha aquatica* var. citrata, *Lamiaceae*) glandular trichomes. Isr J Plant Sci 56:233–244